Journal of Inorganic and Organometallic Polymers and Materials (2018) 28:2100–2107
https://doi.org/10.1007/s10904-018-0865-0

PAMAM Dendrimer Functionalized Manganese Ferrite Magnetic Nanoparticles: Microwave-Assisted Synthesis and Characterization

Ali Serol Ertürk[1] · **Gökhan Elmacı**[2]

Received: 12 March 2018 / Accepted: 28 April 2018 / Published online: 3 May 2018

Abstract
The present study describes the use of microwave-assisted technology for poly(amidoamine) dendrimer (PAMAM) generation grafting on magnetic cores. Based on this aim, starting from a manganese ferrite core (MF), microwave-assisted synthesis of a new series of half generation (G0.5–G2.5) and full generation (G1–G3) PAMAM dendrimer functionalized magnetic nanoparticles (PAMAM@MNPs) were accomplished by the repetitive Micheal addition (45 min) and amidation (30 min) reactions in a considerably shorter period of times compared with the previous studies. The synthesized PAMAM@MNPs with MF core (PAMAM@MFs) were characterized by X-ray powder diffractometry, scanning electron microscopy energy-dispersive X-ray spectroscopy, attenuated total Fourier transform infrared spectroscopy (ATR–FTIR), thermal gravimetric analysis (TGA), and vibrating sample magnetometry. The results showed successful growth of PAMAM generations on MF with a spherical and narrow size distribution and considerable superparamagnetic properties. In particular, ATR–FTIR spectra and TGA thermograms of PAMAM@MFs verified the perfect completion of the Micheal addition and amidation reactions. Remarkably, the solubility of PAMAM@MFs in water and organic solvents enhanced as the generation increased. The developed microwave method can be a great potential for the rapid, facile, and green functionalization of PAMAM dendrons on magnetic cores, and thus the resultant materials could be a general interest of various applications, including drug delivery, protein immobilization, catalysis and scavengers.

Keywords Manganese ferrite ($MnFe_2O_4$) · Microwave-assisted synthesis · PAMAM dendrimers · Magnetic nanoparticle

1 Introduction

Magnetic nanoparticles (MNPs) have received much attention in recent years due to their unique features, which offer significant advantages over traditional materials [1, 2]. They can be obtained from various materials such as metals (Fe, Co, Ni), alloys (FePt, CoPt), metal oxides (FeO, Fe_2O_3, Fe_3O_4) or ferrites ($CoFe_2O_4$, $MnFe_2O_4$) [1, 3, 4]. To prevent agglomeration in water and organic solvents, introducing a shell of polymer, carboxylic acid, dendrimer, etc. to the surface of MNPs is of great importance [5–7]. Therefore, there has been a growing interest towards developing a method to coat MNPs for their effective use in several applications involving drug delivery, protein immobilization, magnetic resonance imaging, biocatalysts, and cancer treatment [8–13].

Dendrimers are a new class of polymers with well defined, three dimensional, hyper branched and relatively monodisperse structures. Since their first appearance [14, 15], polyamido amine dendrimers (PAMAMs) are the most widely studied starburst macromolecules and distinguishable from traditional linear polymers by their starburst architectures [16]. Due to their unique structures, good biocompatibilities, high volume of surface functional groups, controllable sizes, and chemical stabilities, PAMAMs have gained considerable attention in several applications, including drug delivery, gene therapy, catalysis, solubility enhancement, sensing, molecular electronics, or nanomedicine [17], and most probably

Electronic supplementary material The online version of this article (https://doi.org/10.1007/s10904-018-0865-0) contains supplementary material, which is available to authorized users.

✉ Ali Serol Ertürk
aserturk@gmail.com

[1] Department of Analytical Chemistry, Faculty of Pharmacy, Adıyaman University, 02040 Adıyaman, Turkey

[2] Department of Chemistry, Adıyaman University, 02040 Adıyaman, Turkey

they can incorporate their fascinating properties for the construction of PAMAM dendrimer functionalized MNPs (PAMAM@MNPs) [7].

Surface modification or coating of MNPs with PAMAMs can allow the control of the nanocomposite solubility and improve the dispersion in organic solvents by multiplying surface functional groups. Based on this aim, Alper et al. [44] reported a method of growing PAMAMs on the surface of (3-aminopropy)triethoxysilane (APTMS) functionalized SiO_2@Fe_3O_4 MNPs using divergent synthesis approach consisting of the successive reactions of Micheal addition (5 days) and amidation (5 days) to reach half (G0.5–G2.5) and full generations (G1–G3), respectively. Alternatively, Gunduz and co-workers [18] reported those results as 7 and 3 h using ultrasonification technology. Recently, Yang and co-workers [8] have offered microwave heating as a new protocol to improve the long reaction times of PAMAM@MNPs. Nevertheless, their results were 6 h (half generation) and 8 h (full generation). Although microwave approach is interesting, its performance still needs to be improved for the efficient, simple and fast synthesis of PAMAM@MNPs.

Reaction proceedings can be accelerated in microwave-assisted synthesis (MAS) due to the dominant factors, which are selective heating of absorbing species and super heating of solvents under ambient pressure and standard temperature [19]. MAS could reveal the abilities of some liquids or solids while transforming electromagnetic radiation into heat. Over the last decades, an extensive study has been conducted on the development of microwave absorbing species with high magnetic and dielectric loss [20–22]. One of the most popular candidates of these materials is ferrites due to their ease of preparation, specific resistance, and magnetic properties [23]. However, spinel ferrites have been facilitated as the most frequent absorbing species in several forms [24]. In particular, manganese ferrite ($MnFe_2O_4$) has been shown as useful microwave absorbing materials depending on their microwave properties over pure ferrites [25, 26]. Up to present, PAMAM@MNPs have been synthesized starting from pure ferrites or silica-coated MNPs [18, 27, 28, 44]. However, no one as far as we know has studied for the preparation of PAMAM@MNPs by using a magnetic manganese ferrite core (MF).

This study presents a novel MAS method for the preparation of PAMAM@MNPs. For this purpose, microwave-assisted reactions for both half generations (Micheal addition) and full generations (amidation) under a series of different operating trial conditions were performed, and the best reaction conditions were optimized. As a result, a new MAS method was developed and applied for the successful synthesis of a new series of half generation (G0.5–G2.5) and full generation (G1–G3) PAMAM@MNPs starting from a magnetic core $MnFe_2O_4$ and improving the reaction times considerably compared to previous studies.

2 Experimental

2.1 Materials

Methyl acrylate, ethylene diamine, toluene and methanol were purchased from Merck & Co. (Kenilworth, NJ). The reagent grade chemicals, ethylene glycol (Merck), polyvinylpyrrolidone (PVP; BASF, average molecular weight 38,000 Da), $MnSO_4{\cdot}H_2O$ (Merck), $Fe(NO_3)_3{\cdot}9H_2O$ (Applichem), sodium acetate anhydrous (Merck), 3-aminopropyltrimethoxysilane (APTMS) (Sigma-Aldrich, St. Louis, USA) were used as received. Unless otherwise stated, all the other chemicals were obtained from Merck and used as received without further purification. Microwave reactions were performed in sealed heavy-walled 10 mL Pyrex tubes (CEM Corporation, North Carolina, USA).

2.2 Instrumentation

Microwave-irradiated reactions were conducted with a microwave reactor (Discover SP, CEM, Matthews, NC, USA) having a continuous microwave power delivery system with an operator selectable power output from 0 to 300 W (± 30 W) programmable in 1-W increments, infrared temperature control system programmable from 25 to 250 °C, pressure control, and a vessel's capacity of 5 to 125 mL.

Powder X-ray diffraction (XRD) patterns were recorded using a Rigaku D/MAX-2200 diffractometer equipped with graphite-filtered Cu Kα radiation (λ = 1.54056 Å) from 3° to 70° (2θ) at a scanning rate of 2 °C min^{-1}.

The IR (ATR) spectra (4000–650 cm^{-1}, resolution 4 cm^{-1}) were recorded in a PerkinElmer Spectrum 100 FT-IR Spectrometer in order to investigate the formation of the chemical bonds.

TGA thermograms were recorded on a TG-TGA instrument (TA Instruments, New castle, DE) calibrated with indium. Samples were heated from 40 to 800 °C at a scanning rate of 20 °C min^{-1} under a nitrogen flow of 100 mL min^{-1}.

Microscopic characterization and the morphologies of samples were observed by field-emission scanning electron microscopy (SEM) (EVO 10, Carl Zeiss Germany) combined with energy-dispersive X-ray spectroscopy (EDX). Sample analyses were performed at 20 kV under vacuum (about 1×10^{-7} Pa in the source and 7×10^{-5} Pa in the sample chamber).

Magnetisms of the samples were measured at room temperature with a vibrating sample magnetometer (VSM) (Ouantum Designed Physical Property Measurement System) in a magnetic-field range of (30 kOe).

2.3 Synthesis of MNPs

MF was synthesized using a slightly modified hydrothermal method that we previously reported [29]. In a typical procedure, 4 mmol of $MnSO_4$ and 8 mmol of $Fe(NO_3)_3{\cdot}9H_2O$ were dissolved in 50 mL of ethylene glycol. Then, 0.40 g of PVP and 0.05 mol of NaOAc were added to the solution at room temperature. The resulting mixture was stirred for 1 h. The homogenized mixture was maintained in Teflon-lined stainless steel autoclave at 200 °C for 5 h. MF particles were separated by a magnet, washed several times with water/ethanol mixture, and then dried in an oven at 70 °C.

2.4 Coating of MNPs with Aminosilane

The MF core (0.5 g) was reacted with a %10 (w:v) solution of APTMS in toluene (5 mL) at 120 °C for 60 min with a high magnetic stirring in the microwave reactor. The resulting APTMS modified APTMS@MF (designated as G0) was washed with methanol several times using magnetic separation and finally sedimented by centrifugation. The precipitated product was placed in a freeze dryer overnight. The obtained final product was used as the precursor G0 in the synthesis procedure of PAMAM@MNPs (Scheme 1).

2.5 MAS of PAMAM@MFs

Dendrimers can be synthesized by divergent or conventional synthesis approaches. In PAMAM dendrimer synthesis, divergent method is used [30]. In the functionalization of MNPs with PAMAM dendrons, we have utilized from the divergent method. This approach involves iteration of the two successive main reactions which are alkylation of the primary amine groups, namely Micheal addition (Step A), and amidation of the resulting ester groups with ethylene diamine (Step B). While Micheal addition reactions produce half generations, amidation reactions drive the full generation PAMAMs. A systematic representation of PAMAM@MNPs G1–G3 was given in Scheme 1.

2.5.1 Step A (Half Generation Production by Micheal Addition Reaction)

10% (v:v) methyl acrylate:methanol solution (5 mL) was added over the obtained G0 and sonicated in an ultrasonic water bath for 5 min at room temperature. The reaction was conducted at standard temperature mode at 100 °C for 45 min with high magnetic stirring in the microwave reactor. Afterwards, the sealed vessel cooled up to room temperature and the seal was opened. The resulting G0.5 was washed with methanol several times using magnetic separation.

2.5.2 Step B (Full Generation Production by Amidation)

Half generation G0.5 was dispersed in 50% (v:v) methanol:ethylenediamine solution (6 mL) by ultrasonifacation at room temperature. Then, 10 mL vessel was sealed, and the suspended mixture was reacted at 125 °C for 30 min with high magnetic stirring in a microwave reactor. The resulting G1 was washed with methanol several times using magnetic separation. Step A and step B were repeated for a different number of cycles to reach the specified higher generation PAMAM@MNPs with MF core (PAMAM@MFs) (Scheme 1.). The purity of the amine terminated PAMAM@MFs were characterized by ATR-FTIR.

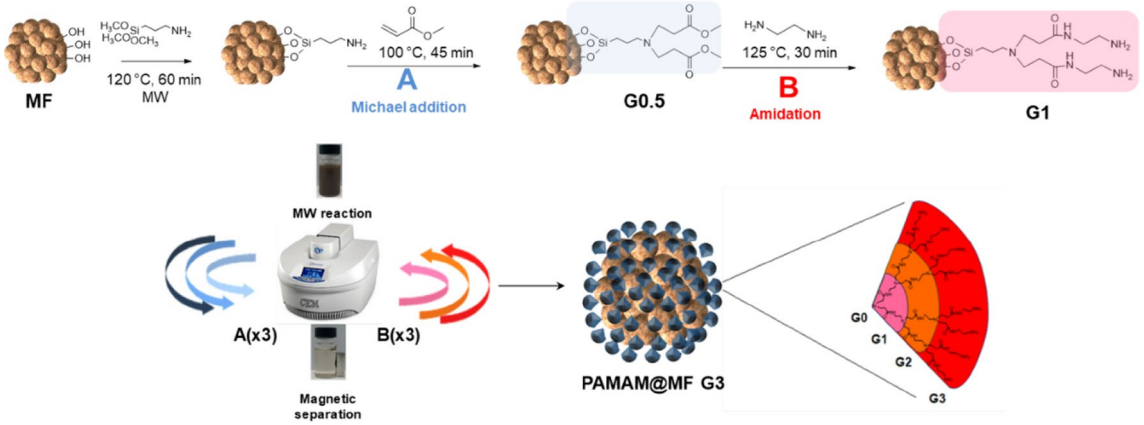

Scheme 1 A systematic representation of PAMAM generation growth on MF

3 Results and Discussion

3.1 MAS of PAMAM@MFs

All the reactions were carried out by microwave irradiation and monitored by ATR-FTIR. Preliminary experiments, under a different series of temperatures (80–150 °C) and microwave method (open vessel and closed vessel), were performed. As a result, reaction conditions for half generation and full generation PAMAM@MFs were optimized as 100 °C for 45 min and 125 °C for 30 min under microwave closed vessel conditions, respectively (Figs. S1, S2). The purity of the synthesized PAMAM@MFs was followed by ATR–FTIR and discussed detailed in the related part. In the ATR monitoring, the full disappearance of the esteric peak at 1734 cm^{-1} was an evidence to precise conversion of the half generations to the full generations and completion of the amidation reactions. In particular, it was observed that the solubility of PAMAM@MFs in water and organic solvents enhanced as the generation increased.

3.2 XRD Analysis

Figure 1 shows the XRD patterns of the MF sample before and after coating with PAMAM. The patterns for MF were referred to the published data [31] and characterized as manganese spinel ferrite (JCPDS 17-465) nanoparticles. All XRD peaks at 2 theta degree = 18.3°, 30.2°, 35.5°, 43.1°, 53.5°, 57.0° and 62.6° for PAMAM@MF G3 nanocomposite were observed in a good agreement with the XRD peaks of pure $MnFe_2O_4$. These peaks correspond to (111), (220), (311), (222), (400), (422), (511), and (440) reflection peak of MF, respectively, indicating that the G3 nanocomposite contain MF particles. PAMAM@MF G3 displayed only core reflections, the shell peaks were not observed because of the relatively thin layer and amorphous form of PAMAM structure.

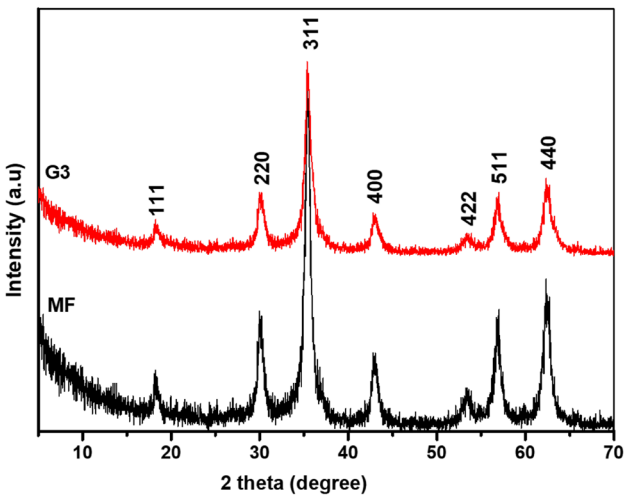

Fig. 1 Powder XRD patterns of the magnetic core (MF) and PAMAM@MF G3

3.3 ATR–FTIR Analysis

ATR–FTIR is a useful and important technique for the characterization of the functional groups of MF [32]. Functionalization of the MF with APTMS and growth of the PAMAM dendrons was monitored by ATR–FTIR and further confirmed by TGA. Figure 2 demonstrates the ATR–FTIR spectra of uncoated MF and APTMS coated APTMS@MF MNPs (G0), half generation G0.5–G2.5 and full generation G1–G3 PAMAM@MNPs. Prominent characteristic peaks in the ATR–FTIR spectra of pure MF were 3442, 1626 and 1315 cm^{-1} which are stemming from OH bending (revealing residual hydrolysis groups) of MF, and C=0 stretching and $–CH_2$ wagging of the residual PVP molecules that are encapsulated between the MF clusters of the magnetic core, respectively [5].

High density of hydroxyl groups provides MF MNPs with excellent aqueous dispersibility to react with the APTMS precursors. There were new absorption bands in the ATR–FTIR spectra of G0 compared with the spectrum of pure MF. The peaks at 1048 and 1111 cm^{-1} show stretching vibration of Si–O and Si–C, respectively, and prove the binding of APTMS on the magnetite surface [33]. Furthermore, the bands at 2860 and 2928 cm^{-1} correspond to symmetric and asymmetric CH_2 bonds on aminopropyl groups. The broad peak at 3342 cm^{-1} indicates the NH_2 bending of APTMS [34–36].

In the spectra of half generations (G0.5–G2.5), the band at 1734 cm^{-1} is a characteristic band that can be attributed to C=O stretching of the ester ($–OCH_3$) functional groups. Disappearance of this band and the occurrence of the peaks at 1585 and 1634 cm^{-1}, which can be assigned to N–H bending/C–N stretching (amide II) and C–O stretching (amide I) vibration of PAMAM dendrimers [5, 37], are of the evidence of the perfection of the amidation reaction and precise conversion of half generations (G0.5–G2.5) to full generations (G1–G3). Amide I and II bands overlap with the residual C=O peak from the encapsulated PVP in MF cluster. However, amide II band gives a shoulder and becomes clearer as the generation growths. The bands between the 2800–3000 cm^{-1} are characteristic of C–H stretching of the methyl and methylene groups [38–40]. In addition, the peaks at 3334 and 3249 cm^{-1} are due to the vibrations of the $–NH_2$ groups in the ATR–FTR spectra of G1–G3 [39, 41]. All these results suggested that MAS of the APTMS grafting, Micheal addition and amidation were achieved.

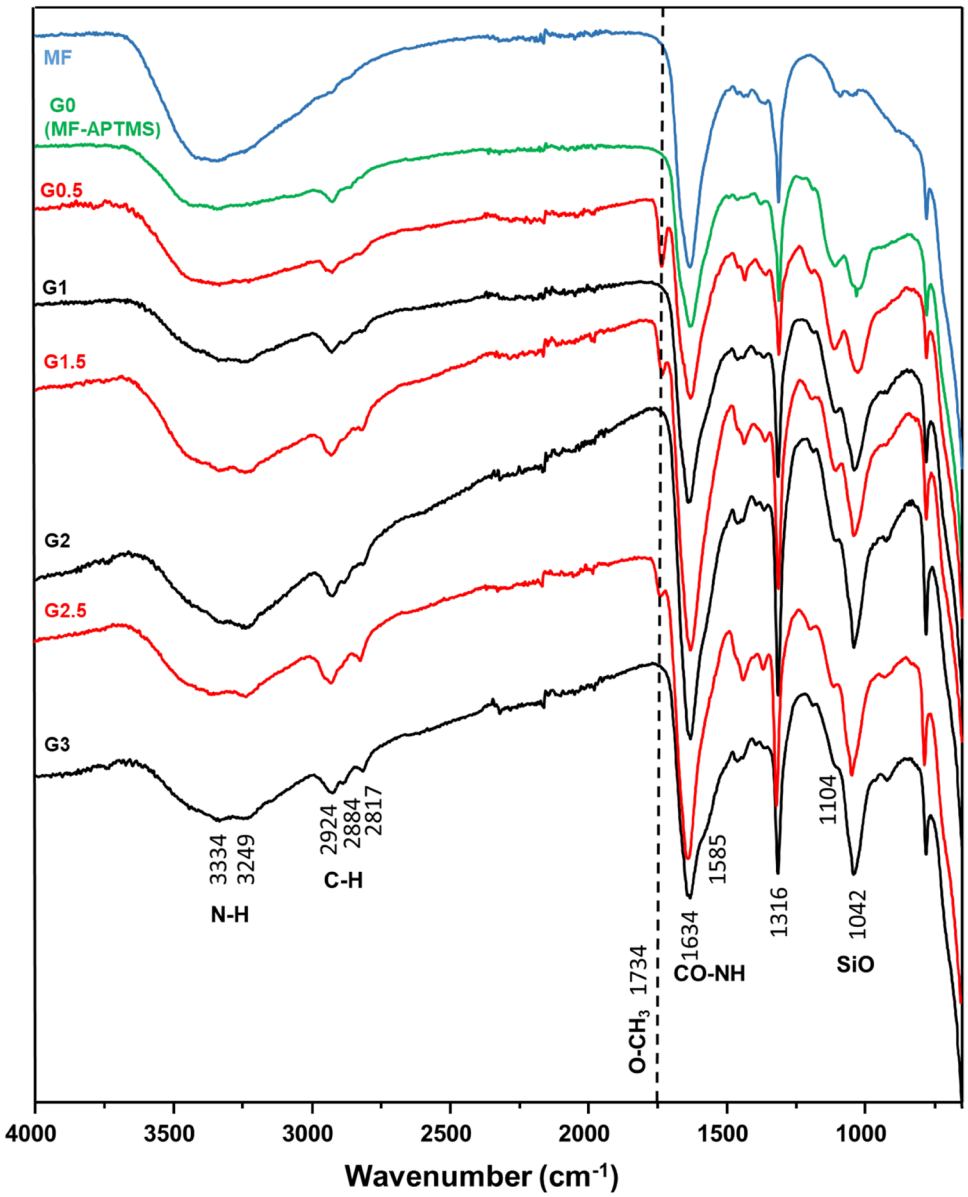

Fig. 2 ATR–FTIR spectra of MF, APTMS@MF and PAMAM@MNPs

3.4 Thermal Analysis

Coating of magnetic core MF with PAMAM can be followed by using TGA. The thermal degradation of the coated MF was similar to the previous studies on the synthesized PAMAM dendrimer nanocomposites [42–44]. To get a better insight into coating process, Thermal behaviors of lower generation G1 and the highest generation G3 were investigated and compared with the magnetic core MF (Fig. 3). TGA thermograms of composites exhibited multiple-step mass losses. As it can be seen from Fig. 3, mass loss up to 160 °C was driven from physically adsorbed water while mass loss between 160 and 420 °C could be attributed to dendritic structure. The amount of organic matter for G1 and G3 PAMAM@MFs was calculated as 5.63 and 6.44% from 160 to 420 °C, respectively. These results revealed that as the number of dendrimer generation increased the percent mass loss was increased.

3.5 SEM and EDX Analysis

In order to analyze the surface morphology and the size distribution, the SEM analysis of MF and PAMAM@MF G3 was performed. The SEM images and the particle size distributions were given in Fig. 4. Investigation of the Fig. 4 revealed that the PAMAM@MF G3 was well dispersed with spherical morphology with an average particle size of 167 nm compared to that of MF, which was 147 nm. Also, polydispersity indexes were calculated by a gauss fit as 14.22% (MF) and 15.86% (PAMAM@MF G3). These

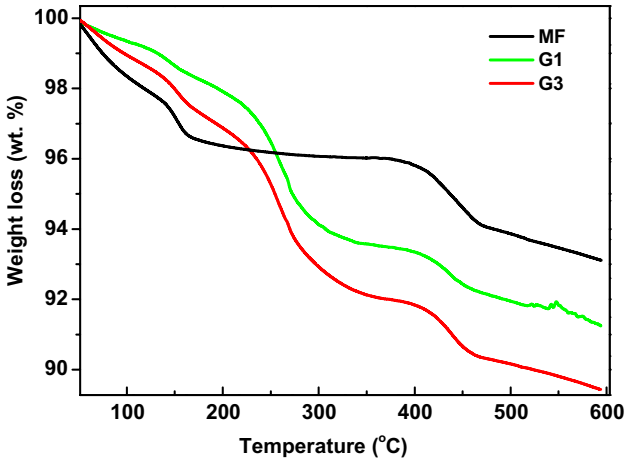

Fig. 3 TGA curves of MF and PAMAM@MF G1 and G3

results suggested that PAMAM@MFs were successfully prepared.

SEM–EDX was applied to show the presence of APTMS thin layer on PAMAM@MFs. Elemental analysis was carried out by positioning at various particles of PAMAM@MF G3. Inspection of Fig. 5 confirmed the presence of Si atoms on the surface of G3.

3.6 Magnetic Measurements

Magnetic properties of PAMAM@MFs were determined by VSM at room temperature. The obtained results indicated that the MF core and PAMAM@MFs G1–G3 exhibited magnetic saturation values in the decreasing order of 50.5, 49.4, 48.3, and 47.5 emu g^{-1}, respectively as the generation increases (Fig. 6). That is, the magnetization of PAMAM@MF nanocomposites decreases regularly depending on the presence of nonmagnetic organic layer on the MF surface as in good correlation with the literature [18, 28, 42]. The PAMAM@MFs showed typical super paramagnetic behavior due to no hysteresis and coercivity [45]. Thus, these particles could be fully dispersed into the solution and then conveniently removed from the suspended solution by external magnet (Fig. 6).

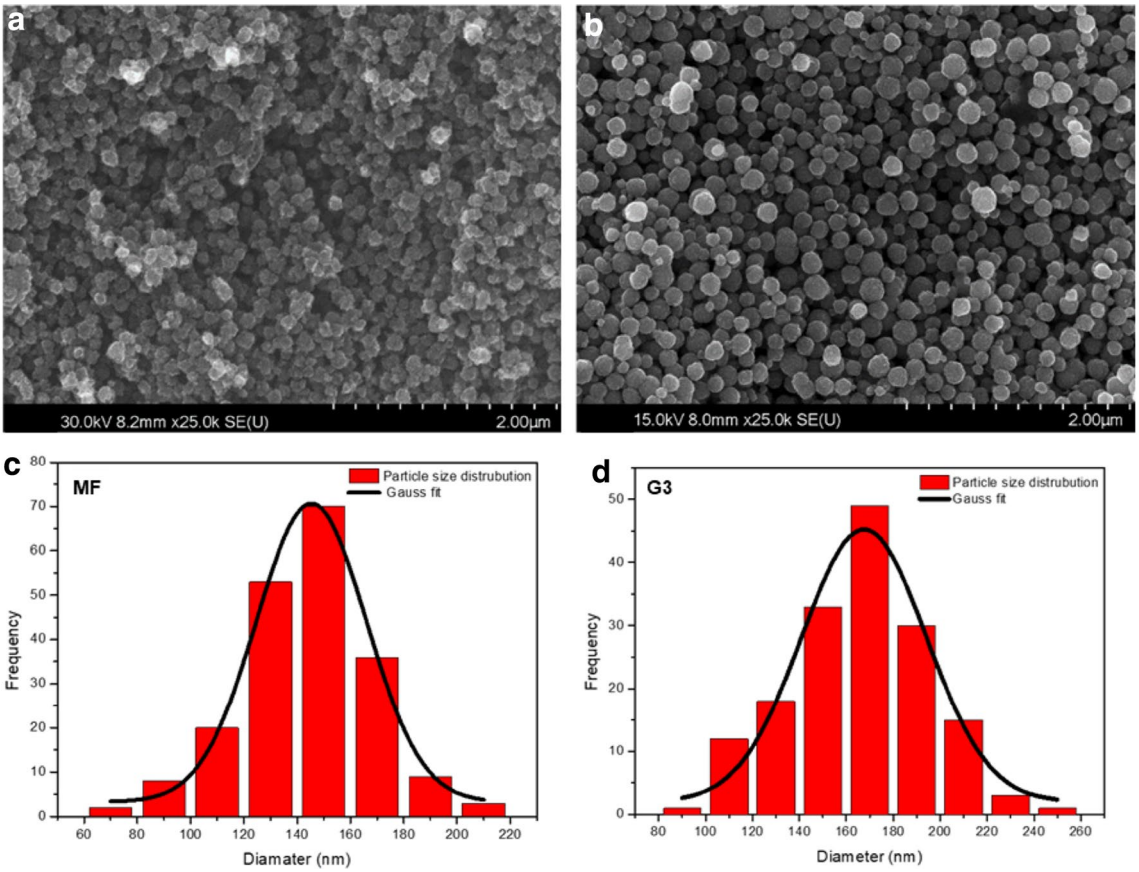

Fig. 4 SEM images of MF (**a**), PAMAM@MF G3 (**b**), particle size distribution diagrams of MF (**c**), and PAMAM@MF G3 (**d**)

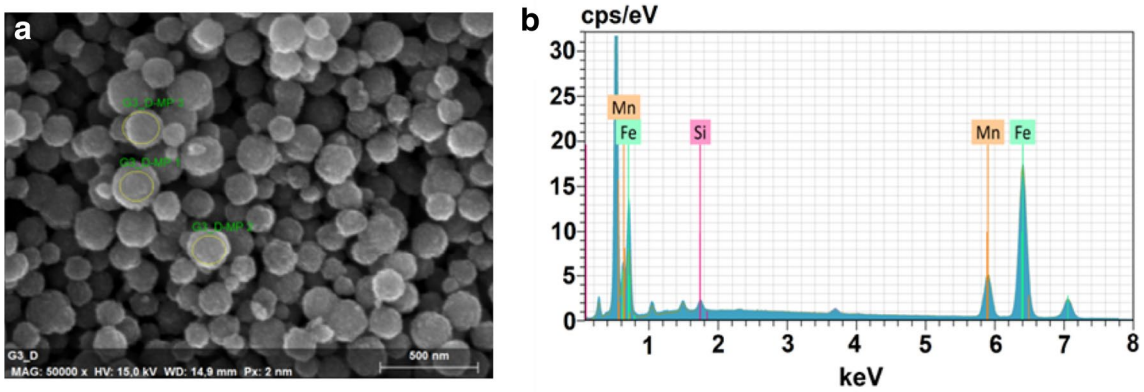

Fig. 5 SEM–EDX image (**a**) and elemental analysis (**b**) of PAMAM@MF G3

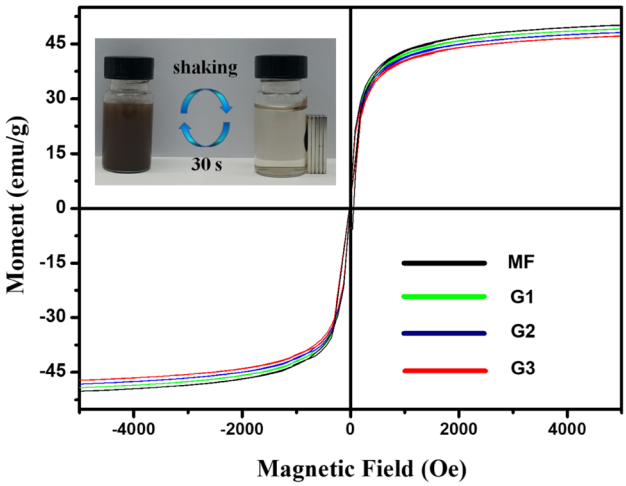

Fig. 6 Magnetization curves of MF and PAMAM@MFs at room temperature

3.7 Comparison of the Reaction Time with the Previous Methods

The current microwave-assisted protocol accelerated the reactions compared to the previous methods. Investigation of the Table 1 revealed that conventional functionalization of MNPs for the half generation and the full generation PAMAM@MNPs required times between 24 h to 5 days and 48 h to 5 days, respectively. On the other hand, sonification improved half generation (7 h) and full generation (3 h) period of reactions. In the present study, those times lowered up to 45 and 30 min, respectively. Obtained results indicated that the current method can be a great potential enhancing the reaction rates for the future studies using PAMAM@MNPs in a wide range of applications including drug delivery, catalysis, scavengers, and many more.

4 Conclusion

A new type of PAMAM@MNPs with MF core up to three generations was synthesized via microwave-assisted technology. In this way, reaction times were reduced considerably for half generation (45 min) and full generation (30 min) PAMAM@MNPs when compared with the previous synthesis methods. XRD, ATR–FTIR, TGA, SEM and EDX analysis confirmed the presence of PAMAM generations on

Table 1 Comparison of the current method with the previous studies for the synthesis PAMAM@MNPs

Magnetic precursos	Synthesis method	Synthesis instrument	Half generation		Full generation		References
			Temp (°C)	Time	Temp (°C)	Time	
SiO_2@Fe_3O_4	Conventional	Conventional	50	5 days	50	5 days	[44]
SiO_2@Fe_3O_4	MW-OV[a]	Discover-SP	50	6–8 h	50	8–12 h	[27]
Fe_3O_4	Conventional	Conventional	40	24 h	–	48 h	[28]
Fe_3O_4	Sonification	Ultrasonic water bath	r.t.	7 h	r.t	3 h	[18]
SiO_2@Fe_3O_4	MW-OV	Discover SP	50	6 h	50	8 h	[8]
$MnFe_2O_4$	MW-CV[b]	Discover-SP	100	45 min	125	30 min	This work

[a]Microwave open vessel

[b]Microwave closed vessel

the MF. The synthesized PAMAM@MFs were spherical, with narrow size distribution. VSM studies showed that all PAMAM@MFs exhibited super magnetic properties. As a result, the current MAS method can be a great potential for the rapid synthesis of magnetic core nanoparticles with PAMAM shell, which have a wide range of interest in several applications involving drug delivery, protein immobilization, catalysis, scavengers and many more.

Acknowledgements This research has been supported by Adıyaman University Scientific Research Projects Coordination Department. (Project Number: MÜFMAP/2015-0004).

Compliance with Ethical Standards

Conflict of interest There is no conflict of interest.

References

1. A.H. Lu, E.L. Salabas, F. Schuth, Angew. Chem. (Int. Ed. in English) **46**, 1222 (2007)
2. J. Kudr, Y. Haddad, L. Richtera, Z. Heger, M. Cernak, V. Adam, O. Zitka, Nanomaterials **7**, 243 (2017)
3. V. Polshettiwar, R. Luque, A. Fihri, H. Zhu, M. Bouhrara, J.M. Basset, Chem. Rev. **111**, 3036 (2011)
4. S. Shylesh, V. Schünemann, W.R. Thiel, Angew. Chem. Int. Ed. **49**, 3428 (2010)
5. M. Tajabadi, M.E. Khosroshahi, S. Bonakdar, Colloids Surf. A **431**, 18 (2013)
6. B. Garlyyev, Z. Durmus, N. Kemikli, H. Sozeri, A. Baykal, R. Ozturk, Polyhedron **30**, 2843 (2011)
7. Q.M. Kainz, O. Reiser, Acc. Chem. Res. **47**, 667 (2014)
8. Y. Wang, P. Su, S. Wang, J. Wu, J. Huang, Y. Yang, J. Mater. Chem. B **1**, 5028 (2013)
9. M. Răcuciu, D.E. Creangă, A. Airinei, Eur. Phys. J. E **21**, 117 (2006)
10. D.L. Zhao, X.W. Zeng, Q.S. Xia, J.T. Tang, J. Alloy. Compd. **469**, 215 (2009)
11. H. Nosrati, M. Adibtabar, A. Sharafi, H. Danafar, M. Hamidreza Kheiri, Drug Dev. Ind. Pharm. (2018). https://doi.org/10.1080/03639045.2018.1451881
12. N. Taghavi Pourianazar, U. Gunduz, Biomed. Pharmacother. **78**, 81 (2016)
13. A. Boni, A.M. Basini, L. Capolupo, C. Innocenti, M. Corti, M. Cobianchi, F. Orsini, A. Guerrini, C. Sangregorio, A. Lascialfari, RSC Adv. **7**, 44104 (2017)
14. G.R. Newkome, Z.Q. Yao, G.R. Baker, V.K. Gupta, J. Org. Chem. **50**, 2003 (1985)
15. D.A. Tomalia, H. Baker, J. Dewald, M. Hall, G. Kallos, S. Martin, J. Roeck, J. Ryder, P. Smith, Polym. J. **17**, 117 (1985)
16. R. Esfand, D.A. Tomalia, Drug Discov. Today **6**, 427 (2001)
17. E. Abbasi, S.F. Aval, A. Akbarzadeh, M. Milani, H.T. Nasrabadi, S.W. Joo, Y. Hanifehpour, K. Nejati-Koshki, R. Pashaei-Asl, Nanoscale Res. Lett. **9**, 247 (2014)
18. R. Khodadust, G. Unsoy, S. Yalcin, G. Gunduz, U. Gunduz, J. Nanopart. Res. **15**, 1488 (2013)
19. S. Sinnwell, H. Ritter, Aust. J. Chem. **60**, 729 (2007)
20. P. Singh, V.K. Babbar, A. Razdan, R.K. Puri, T.C. Goel, J. Appl. Phys. **87**, 4362 (2000)
21. S. Ruan, B. Xu, H. Suo, F. Wu, S. Xiang, M. Zhao, J. Magn. Magn. Mater. **212**, 175 (2000)
22. T. Nakamura, J. Appl. Phys. **88**, 348 (2000)
23. M. Pardavi-Horvath, J. Magn. Magn. Mater. **215**, 171 (2000)
24. C.H. Peng, C.C. Hwang, J. Wan, J.S. Tsai, S.Y. Chen, Mater. Sci. Eng. B **117**, 27 (2005)
25. K.J. Vinoy, R.M. Jha, *Radar Absorbing Materials* (Kluwer Academic Publishers, Boston, 1996)
26. H.M. Xiao, X.M. Liu, S.Y. Fu, Compos. Sci. Technol. **66**, 2003 (2006)
27. J. Huang, P. Su, L. Zhou, Y. Yang, Colloids Surf. A **490**, 241 (2016)
28. U. Kurtan, S. Esir, A. Baykal, H. Sözeri, J. Supercond. Novel Magn. **27**, 2097 (2014)
29. G. Elmaci, D. Ozer, B. Zumreoglu-Karan, Catal. Commun. **89**, 56 (2017)
30. J.M.J. Fréchet, D.A. Tomalia, *Dendrimers and Other Dendritic Polymers* (Wiley, Chichester, 2001), pp. 587–604
31. G. Elmaci, C.E. Frey, P. Kurz, B. Zumreoglu-Karan, J. Mater. Chem. A **4**, 8812 (2016)
32. B. Sahoo, S.K. Sahu, S. Nayak, D. Dhara, P. Pramanik, Catal. Sci. Technol. **2**, 1367 (2012)
33. P.J. Launer, in *Silicone Compounds Register and Review* (Petrarch Systems, Bristol, 1987), pp. 100–103
34. M. Ma, Y. Zhang, W. Yu, H.Y. Shen, H.Q. Zhang, N. Gu, Colloids Surf. A **212**, 219 (2003)
35. P. Pramanik, S. Mohapatra, N. Pramanik, S. Mukherjee, S.K. Ghosh, J. Mater. Sci. **42**, 7566 (2007)
36. M. Yamaura, R.L. Camilo, L.C. Sampaio, M.A. Macêdo, M. Nakamura, H.E. Toma, J. Magn. Magn. Mater. **279**, 210 (2004)
37. A.S. Ertürk, M. Tülü, A.E. Bozdoğan, T. Parali, Eur. Polym. J. **52**, 218 (2014)
38. A. Baykal, M.S. Toprak, Z. Durmus, M. Senel, H. Sozeri, A. Demir, J. Supercond. Novel Magn. **25**, 1541 (2012)
39. B. Pan, D. Cui, Y. Sheng, C. Ozkan, F. Gao, R. He, Q. Li, P. Xu, T. Huang, Cancer Res. **67**, 1856 (2007)
40. N. Tsubokawa, T. Takayama, React. Funct. Polym. **43**, 341 (2000)
41. C.M. Chou, H.L. Lien, J. Nanopart. Res. **13**, 2099 (2011)
42. U. Kurtan, A. Baykal, H. Sözeri, J. Inorg. Organomet. Polym. Mater. **24**, 948 (2014)
43. N. Dayyani, A. Ramazani, S. Khoee, A. Shafiee, Silicon **10**, 595 (2018)
44. R. Abu-Reziq, H. Alper, D. Wang, M.L. Post, J. Am. Chem. Soc. **128**, 5279 (2006)
45. S. Gautam, P. Shandilya, B. Priya, V.P. Singh, P. Raizada, R. Rai, M.A. Valente, P. Singh, Sep. Purif. Technol. **172**, 498 (2017)